On the Dynamic Response of a Thin Cylindrical Shell to Pulse Loading

Toshihiro IRIE*, Gen YAMADA* and Yasuo YANAGI*

(Received October 29, 1973)

Abstract

According to Flügge's method, the equations of motion are derived, for the purpose of theoretical studies of the deflection and stress of thin cylindrical shell caused by pulse load acting on a narrow surface. The solution is expressed by Fourier series in a general form which can be applied to the studies of the dynamic response to any transient loading under arbitrary boundary conditions. The response function is obtained on a circular cylindrical shell with a simple support at both ends, when the half-sinusoidal side pressure acts inwards on a square surface area located at the midpoint of the cylinder.

The following conclusions are obtained from the numerical calculation based on the theory. Tensile stress occurs on the inner surface and compressive stress occurs on the outer surface. The maximum deflection and stresses occur immediately after the end of loading and remarkable deformation and stresses are produced in a range of two or three fold loaded surface during a double loading period. When the duration of loading becomes short, the deflection and stress levels increase and the time at which the maximum stresses occur becomes fast. The result of the numerical calculation agrees with that of the experiment qualitatively.

1. Introduction

The vibration problems on cylindrical shells have been studied since Lord Rayleigh in 1889[1,2]. Recently these problems are attracting increasing interest for structural engineers, and the theories on a thin cylindrical shell, which is the most simple and typical model of shell structures, have been developed in various fields including mechanical engineering.

The typical methods for deriving the equations of motion for a thin cylindrical shell are described in Flügge's book[3] and Donnell's paper[4]. Arnold-Warburton[5,6], Baron-Bleigh[7], Yu[8,9], Forsberg[10] and others have studied the natural vibration of thin shells on the basis of the equations. Humphreys-Winder[11] and Sheng[12] analyzed the dynamic response to pulse loading distributed over the entire surface of the shells. However, there are only a few studies available on the response of the shells to side pressure pulse acting on a restricted surface.

In this paper, the deformation and the stress of an elastic thin cylindrical shell produced by a pulse pressure acting on a narrow surface, were analyzed theoretically with the aid of Fourier series which satisfies the equations of motion derived by Füge's method. The result of the theoretical calculation is compared with that of an experiment.

* Department of mechanical Engineering II, Hokkaido University, Japan

Notations

The following notations are used to denote the dimensions, the components of displacement, forces, moments, and characteristic values of the shell.

a^* : mean radius, h^* : thickness, l^* : full length, x^* : distance in the axial direction, z^* : distance in radial direction, ϕ : angle in a plane perpendicular to the axis, t : time.

(u^*, v^*, w^*) : displacement, $(\varepsilon_x, \varepsilon_\phi)$: normal strain, $\gamma_{x\phi}$: shearing strain, $(\sigma_x^*, \sigma_\phi^*)$: normal stress, $\tau_{x\phi}^*$: shearing stress, (p_x^*, p_ϕ^*, p_r^*) : pulse loading (side pressure), $(N_x, N_\phi, N_{x\phi}, N_{\phi x})$: normal force, (Q_x, Q_ϕ) : shearing force, (M_x, M_ϕ) : bending moment, $(M_{x\phi}, M_{\phi x})$: torsional moment.

ρ : density, E : modulus of elasticity, ν : Poison's ratio, $D=Eh^{*3}/\{12(1-\nu^2)\}$: rigidity in deflection, $K=Eh^*/(1-\nu^2)$: rigidity in elongation.

The dimensionless notations are used for the convenience of theoretical analysis.

$h=h^*/a^*$, $l=l^*/a^*$, $x=x^*/a^*$, $z=z^*/a^*$, $\tau=t/\{a^*\sqrt{\rho(1-\nu^2)/E}\}$, $(u, v, w)=(u^*, v^*, w^*)/a^*$, $(\sigma_x, \sigma_\phi)=(\sigma_x^*, \sigma_\phi^*)/\{E/(1-\nu^2)\}$, $\tau_{x\phi}=\tau_{x\phi}^*/[E/\{2(1+\nu)\}]$, $(p_x, p_\phi, p_r)=(p_x^*, p_\phi^*, p_r^*)/[Eh^*/\{a^*(1-\nu^2)\}]$, (ξ, ξ_0) : location and range of loading, ϕ_0 : range (angle) of loading, f_0 : the maximum value of half-sinusoidal loading, τ_1 : duration of loading, τ_2 : straight-line rise time of step-force.

$\omega_{mn}^{(r)}$: natural frequency, $k=(1/12)(h^*/a^*)^2$

It is convenient to use the symbols for the simplification of the description.

$'=\partial/\partial x$: partial derivative with respect to x, $\cdot=\partial/\partial\phi$: partial derivative with respect to ϕ, $\{\ \}$: column vector, $[\ ]$: square matrix.

2. The equations of motion of an elastic thin shell

The components of the displacement of a circular cylindrical shell and the forces and moments acting on the element are shown in Figs. 1 and 2. These components are taken as positive in the direction indicated in the figures. If the small terms can be neglected under the assumption that the deformation of the shell is small, the following equations of motion are obtained from the equilibrium condition of the forces and moments.

$$\left.\begin{aligned} &N_x'+N_{\phi x}'+a^*p_x^*=\rho a^*h^*\frac{\partial^2 u^*}{\partial t^2}\\ &N_\phi'+N_{\phi x}'-Q_\phi+a^*p_\phi^*=\rho a^*h^*\frac{\partial^2 v^*}{\partial t^2}\\ &Q_\phi'+Q_x'+N_\phi-a^*p_r^*=-\rho a^*h^*\frac{\partial^2 w^*}{\partial t^2}\end{aligned}\right\} \qquad (1)$$

and

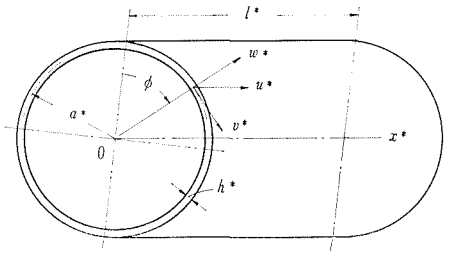

Fig. 1 A thin cylindrical shell

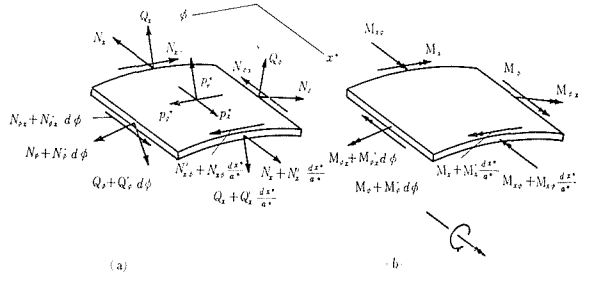

Fig. 2 Forces and moments acting on element

$$\left.\begin{aligned} &M_x'+M_{\phi x}'-a^*Q_x=0, \qquad M_\phi'+M_{x\phi}'-a^*Q_\phi=0\\ &a^*N_{x\phi}-a^*N_{\phi x}+M_{\phi x}=0 \end{aligned}\right\} \tag{2}$$

where the notations $'$ and $\cdot$ denote the partial derivatives with respect to x^*/a^* and ϕ respectively. The strain components are written by

$$\left.\begin{aligned} &\varepsilon_x=\frac{u^{*\prime}}{a^*}-z^*\frac{w^{*\prime\prime}}{a^{*2}}, \qquad \varepsilon_\phi=\frac{v^{*\cdot}}{a^*}-\frac{z^*}{a^*}\frac{w^{*\cdot\cdot}}{a^*+z^*}+\frac{w^*}{a^*+z^*}\\ &\gamma_{x\phi}=\frac{u^{*\cdot}}{a^*+z^*}+\frac{a^*+z^*}{a^{*2}}v^{*\prime}-\frac{w^{*\prime\cdot}}{a^*}\left(\frac{z^*}{a^*}+\frac{z^*}{a^*+z^*}\right) \end{aligned}\right\} \tag{3}$$

under the assumption that a plane which was perpendicular to the neutral surface before deformation continues to remain in a plane after deformation and the thickness of the shell is not varied by the deformation (Kirchhoff-Love's assumption).

The forces and moments acting on the element are expressed by the stress components, which are written by the strain components according to Hooke's law. Since the strain is expressed by the displacement as shown in Eq. (3), the forces and moments are written by only the displacement. By substituting Q_x, Q_ϕ obtained from the first two equations of Eq. (2) in Eq. (1), the forces Q_x, Q_ϕ can be eliminated. And by substituting the forces N_x, N_ϕ, $N_{x\phi}$, $N_{\phi x}$ and the moments M_x, M_ϕ, $M_{x\phi}$, $M_{\phi x}$ expressed by the components of the displacement in Eq. (1), the following equations of motion are obtained.

$$\left.\begin{aligned} &D\left(u^{*\prime\prime}+\frac{1-\nu}{2}u^{*\cdot\cdot}+\frac{1+\nu}{2}v^{*\prime\cdot}+\nu w^{*\prime}\right)\\ &\qquad+\frac{K}{a^{*2}}\left(\frac{1-\nu}{2}u^{*\cdot\cdot}-w^{*\prime\prime\prime}+\frac{1-\nu}{2}w^{*\prime\cdot\cdot}\right)+a^{*2}p_x^*=\rho h^*a^{*2}\frac{\partial^2u^*}{\partial t^2}\\ &D\left(\frac{1+\nu}{2}u^{*\prime\cdot}+v^{*\cdot\cdot}+\frac{1-\nu}{2}v^{*\prime\prime}+w^{*\cdot}\right)\\ &\qquad+\frac{K}{a^{*2}}\left(\frac{3}{2}(1-\nu)v^{*\prime\prime}-\frac{3-\nu}{2}w^{*\prime\prime\cdot}\right)+a^{*2}p_\phi^*=\rho h^*a^{*2}\frac{\partial^2v^*}{\partial t^2}\\ &D(\nu u^{*\prime}+v^{*\cdot}+w^*)+\frac{K}{a^{*2}}\left(\frac{1-\nu}{2}u^{*\prime\cdot\cdot}-u^{*\prime\prime\prime}-\frac{3-\nu}{2}v^{*\prime\prime\cdot}+w^{*\prime\prime\prime\prime}\right.\\ &\qquad\left.+2w^{*\prime\prime\cdot\cdot}+w^{*\cdot\cdot\cdot\cdot}+2w^{*\cdot\cdot}+w^*\right)-a^{*2}p_r^*=-\rho h^*a^{*2}\frac{\partial^2w^*}{\partial t^2} \end{aligned}\right\} \tag{4}$$

If the small terms are neglected, the last equation of Eq. (2) can be automatically satisfied. It is convenient to write Eq. (4) in the dimensionless form

$$\begin{pmatrix} L_{11} & L_{12} & L_{13}\\ L_{21} & L_{22} & L_{23}\\ L_{31} & L_{32} & L_{33}\end{pmatrix}\begin{Bmatrix} u\\ v\\ w\end{Bmatrix}=-\begin{Bmatrix} p_x\\ p_\phi\\ -p_r\end{Bmatrix} \tag{5}$$

where L_{ij} is the partial derivatives expressed by

$$\left.\begin{aligned} &L_{11}=\frac{\partial^2}{\partial x^2}+(1+k)\frac{1-\nu}{2}\frac{\partial^2}{\partial\phi^2}-\frac{\partial^2}{\partial\tau^2}, \qquad L_{22}=\frac{\partial^2}{\partial\phi^2}+(1+3k)\frac{1-\nu}{2}\frac{\partial^2}{\partial x^2}-\frac{\partial^2}{\partial\tau^2}\\ &L_{33}=1+k+k\left(\frac{\partial^2}{\partial x^2}+\frac{\partial^2}{\partial\phi^2}\right)^2+2k\frac{\partial^2}{\partial\phi^2}+\frac{\partial^2}{\partial\tau^2}\\ &L_{12}=L_{21}=\frac{1+\nu}{2}\frac{\partial^2}{\partial\phi\partial x}, \qquad L_{23}=L_{32}=\frac{\partial}{\partial x}-k\frac{3-\nu}{2}\frac{\partial^3}{\partial x^2\partial\phi}\\ &L_{13}=L_{31}=\nu\frac{\partial}{\partial x}-k\frac{\partial^3}{\partial x^3}+k\frac{1-\nu}{2}\frac{\partial^3}{\partial x\partial\phi^2} \end{aligned}\right\} \tag{6}$$

3. The dynamic response of the shell to pulse loading

By using the eigenfunctions (U_{mnf}, V_{mnf}, W_{mnf}) of the shell, the displacement can be written by

$$\begin{Bmatrix} u \\ v \\ w \end{Bmatrix} = \sum_{m=1}^{\infty} \sum_{n=0}^{\infty} \begin{Bmatrix} U_{mna}(x)\cos n\phi + U_{mnb}(x)\sin n\phi \\ V_{mna}(x)\sin n\phi + V_{mnb}(x)\cos n\phi \\ W_{mna}(x)\cos n\phi + W_{mnb}(x)\sin n\phi \end{Bmatrix} e^{j\omega_{mn}\tau} \tag{7}$$

By substituting Eq. (7) in Eq. (5) whose right-hand sides are equal to zero, the equations of the natural vibrations of the shell are obtained as follows.

$$\omega_{mn}^2 \begin{Bmatrix} U_{mnf}(x) \\ V_{mnf}(x) \\ W_{mnf}(x) \end{Bmatrix} = \begin{Bmatrix} -U''_{mnf} + (1+k)\frac{1-\nu}{2}n^2 U_{mnf} \mp \frac{1+\nu}{2}nV'_{mnf} + kW'''_{mnf} + \left(kn^2\frac{1-\nu}{2} - \nu\right)W'_{mnf} \\ \pm\frac{1+\nu}{2}nU'_{mnf} - (1+3k)\frac{1-\nu}{2}V''_{mnf} + n^2 V_{mnf} \mp \left(kn\frac{3-\nu}{2}W''_{mnf} - nW_{mnf}\right) \\ -kU'''_{mnf} + \left(\nu - kn^2\frac{1-\nu}{2}\right)U'_{mnf} \mp \left(kn\frac{3-\nu}{2}V''_{mnf} - nV_{mnf}\right) \\ \qquad + kW''''_{mnf} - 2kn^2 W''_{mnf} + \{1+k(n^2-1)^2\}W_{mnf} \end{Bmatrix}$$
$$(m, n = 0, 1, 2, \ldots;\ f = a, b) \tag{8}$$

where the upper sign is used for $f=a$ and the lower sign for $f=b$ respectively. The displacement is written by

$$\begin{Bmatrix} u \\ v \\ w \end{Bmatrix} = \begin{Bmatrix} u_0(x,\tau) \\ 0 \\ w_0(x,\tau) \end{Bmatrix} + \sum_{n=1}^{\infty} \begin{Bmatrix} u_{na}(x,\tau)\cos n\phi + u_{nb}(x,\tau)\sin n\phi \\ v_{na}(x,\tau)\sin n\phi + v_{nb}(x,\tau)\cos n\phi \\ w_{na}(x,\tau)\cos n\phi + w_{nb}(x,\tau)\sin n\phi \end{Bmatrix} \tag{9}$$

and the side pressure is

$$\begin{Bmatrix} p_x \\ p_\phi \\ p_r \end{Bmatrix} = \begin{Bmatrix} X_0(x,\tau) \\ 0 \\ R_0(x,\tau) \end{Bmatrix} + \sum_{n=1}^{\infty} \begin{Bmatrix} X_{na}(x,\tau)\cos n\phi + X_{nb}(x,\tau)\sin n\phi \\ \Phi_{na}(x,\tau)\sin n\phi + \Phi_{nb}(x,\tau)\cos n\phi \\ R_{na}(x,\tau)\cos n\phi + R_{nb}(x,\tau)\sin n\phi \end{Bmatrix} \tag{10}$$

(u_{nf}, v_{nf}, w_{nf}) and $(X_{nf}, \Phi_{nf}, R_{nf})$ can be represented by

$$\begin{Bmatrix} u_{nf} \\ v_{nf} \\ w_{nf} \end{Bmatrix} = \sum_{m=1}^{\infty} q_{mnf}(\tau) \begin{Bmatrix} U_{mnf}(x) \\ V_{mnf}(x) \\ W_{mnf}(x) \end{Bmatrix}, \quad \begin{Bmatrix} X_{nf} \\ \Phi_{nf} \\ R_{nf} \end{Bmatrix} = \sum_{m=1}^{\infty} Q_{mnf}(\tau) \begin{Bmatrix} U_{mnf}(x) \\ V_{mnf}(x) \\ W_{mnf}(x) \end{Bmatrix} \tag{11}$$

Substituting Eq. (11) in Eq. (5) and rearranging the result by Eq. (8), the following equation is obtained

$$\frac{d^2}{d\tau^2}q_{mnf}(\tau) + \omega_{mn}^2 q_{mnf}(\tau) = Q_{mnf}(\tau) \tag{12}$$

By applying the orthogonality property of the eigenfunctions $(U_{mnf}, V_{mnf}, W_{mnf})$

$$\int_0^l (U_{inf}U_{jnf} + V_{inf}V_{jnf} + W_{inf}W_{jnf})dx = 0 \quad (i \neq j) \tag{13}$$

to Eq. (11), $Q_{mnf}(\tau)$ is given by

$$Q_{mnf}(\tau) = \frac{\int_0^l (X_{nf}U_{mnf} + \Phi_{nf}V_{mnf} + R_{nf}W_{mnf})dx}{\int_0^l (U_{mnf}^2 + V_{mnf}^2 + W_{mnf}^2)dx} \tag{14}$$

The solution of Eq. (12) which is expressed by

$$q_{mnf}(\tau) = q_{mnf}(0)\cos\omega_{mn}\tau + \frac{1}{\omega_{mn}}\frac{d}{d\tau}\left(q_{mnf}(0)\right)\sin\omega_{mn}\tau + \frac{1}{\omega_{mn}}\int_0^\tau Q_{mnf}(\tau')\sin\omega_{mn}(\tau-\tau')d\tau' \tag{15}$$

gives the response functions of the shell. Thus the displacement is obtained by

$$\begin{Bmatrix} u \\ v \\ w \end{Bmatrix} = \sum_{m=1}^{\infty}\sum_{r=1}^{2} q_{m0a}^{(r)} \begin{Bmatrix} \alpha_{m0a}^{(r)}\cos\lambda_m x \\ 0 \\ \sin\lambda_m x \end{Bmatrix} + \sum_{m=1}^{\infty}\sum_{n=1}^{\infty}\sum_{r=1}^{3} q_{mna}^{(r)} \begin{Bmatrix} \alpha_{mna}^{(r)}\cos\lambda_m x\cos n\phi \\ \beta_{mna}^{(r)}\sin\lambda_m x\sin n\phi \\ \sin\lambda_m x\cos n\phi \end{Bmatrix} \tag{16}$$

Since the stress components are given by the displacement in the form

$$\begin{Bmatrix} \sigma_x \\ \sigma_\phi \\ \tau_{x\phi} \end{Bmatrix} = \begin{bmatrix} \dfrac{\partial}{\partial x} & \nu\dfrac{\partial}{\partial \phi} & \dfrac{\nu}{1+z} - z\dfrac{\partial^2}{\partial x^2} - \dfrac{z}{1+z}\nu\dfrac{\partial^2}{\partial \phi^2} \\ \nu\dfrac{\partial}{\partial x} & \dfrac{\partial}{\partial \phi} & \dfrac{1}{1+z} - \nu z\dfrac{\partial^2}{\partial x^2} - \dfrac{z}{1+z}\dfrac{\partial^2}{\partial \phi^2} \\ \dfrac{1}{1+z}\dfrac{\partial}{\partial \phi} & (1+z)\dfrac{\partial}{\partial x} & -\left(z+\dfrac{z}{1+z}\right)\dfrac{\partial^2}{\partial x \partial \phi} \end{bmatrix} \begin{Bmatrix} u \\ v \\ w \end{Bmatrix} \tag{17}$$

by substituting Eq. (16) in Eq. (17), the stress components are written by

$$\begin{Bmatrix} \sigma_x \\ \sigma_\phi \\ \tau_{x\phi} \end{Bmatrix} = \sum_{m=1}^{\infty}\sum_{r=1}^{2} q_{m0a}^{(r)} \sin \lambda_m x \begin{Bmatrix} -\lambda_m \alpha_{m0a}^{(r)} + \lambda_m^2 z + \dfrac{\nu}{1+z} \\ -\lambda_m \nu \alpha_{m0a}^{(r)} + \lambda_m^2 \nu z + \dfrac{1}{1+z} \\ 0 \end{Bmatrix}$$

$$+ \sum_{m=1}^{\infty}\sum_{n=1}^{\infty}\sum_{r=1}^{3} q_{mna}^{(r)} \begin{Bmatrix} \left\{-\lambda_m \alpha_{mna}^{(r)} + \nu n \beta_{mna}^{(r)} + \dfrac{z}{1+z}\nu n^2\right\} \sin \lambda_m x \cos n\phi \\ \left\{-\lambda_m \nu \alpha_{mna}^{(r)} + n\beta_{mna}^{(r)} + \dfrac{z}{1+z} n^2\right\} \sin \lambda_m x \cos n\phi \\ \left\{-\dfrac{n}{1+z}\alpha_{mna}^{(r)} + (1+z)\lambda_m \beta_{mna}^{(r)} + \left(z+\dfrac{z}{1+z}\right) n\lambda_m\right\} \cos \lambda_m x \sin n\phi \end{Bmatrix} \tag{18}$$

The eigenfunctions of a cylindrical shell supported at both ends can be written in the form

$$\begin{Bmatrix} U_{mnf}^{(r)}(x) \\ V_{mnf}^{(r)}(x) \\ W_{mnf}^{(r)}(x) \end{Bmatrix} = \begin{Bmatrix} \alpha_{mnf}^{(r)} \cos \lambda_m x \\ \beta_{mnf}^{(r)} \sin \lambda_m x \\ \sin \lambda_m x \end{Bmatrix} \tag{19}$$

where $\lambda_m = m\pi/l$, and there are three values of r for the (m, n) th mode of vibration respectively. In this case, by substituting Eq. (19) in Eq. (7), the following homogeneous equations are derived.

$$\begin{bmatrix} \omega_{mn}^{(r)2} - \left\{\lambda_m^2 + \dfrac{1-\nu}{2}(1+k)n^2\right\} & \pm\dfrac{1+\nu}{2} n\lambda_m & \nu + k\left(\lambda_m^2 - \dfrac{1-\nu}{2}n^2\right) \\ \pm\dfrac{1+\nu}{2} n\lambda_m & \omega_{mn}^{(r)2} - \left\{n^2 + \dfrac{1-\nu}{2}(1+3k)\lambda_m^2\right\} & \pm n\left(1 + \dfrac{3-\nu}{2}k\lambda_m^2\right) \\ \nu + k\left(\lambda_m^2 - \dfrac{1-\nu}{2}n^2\right) & \mp n\left(1 + \dfrac{3-\nu}{2}k\lambda_m^2\right) & \omega_{mn}^{(r)2} - [1 + k\{\lambda_m^4 + 2n^2\lambda_m^2 + (n^2-1)^2\}] \end{bmatrix}$$

$$\times \begin{Bmatrix} \alpha_{mnf}^{(r)} \\ \beta_{mnf}^{(r)} \\ 1 \end{Bmatrix} = 0 \tag{20}$$

The positive roots of the equation obtained by taking the determinants of the coefficient matrix of Eq. (20) as zero, give the natural frequencies $\omega_{mn}^{(r)}$. It should be noted that there are three natural frequencies in the (m, n) th mode of vibration respectively. By applying $\omega_{mn}^{(r)}$'s values thus obtained to Eq. (20), the coefficients $\alpha_{mnf}^{(r)}$ and $\beta_{mnf}^{(r)}$ are calculated, and hence the eigenfunctions are determined by Eq. (19).

4. The response of the shell simply supported at both ends to side pressure acting on a rectangular surface area

When a side pressure which is expressed by

$$p(x, \phi, \tau) = \begin{cases} p(\tau) & (\xi - \xi_0 \le x/l \le \xi + \xi_0, \quad -\phi_0 \le \phi \le \phi_0) \\ 0 & (0 \le x/l \le \xi - \xi_0, \quad \xi + \xi_0 \le x/l \le 1, \quad \phi_0 \le \phi \le 2\pi - \phi_0) \end{cases} \tag{21}$$

acts on a rectangular surface area along the axial and circumferential direction as shown in Fig. 3, the dynamic response of the shell simply supported at both ends is calculated as follows. Eq. (21) can be expressed by the Fourier series

$$p(x,\phi,\tau)=p(\tau)\frac{4\phi_0}{\pi^2}\sum_{m=1}^{\infty}\frac{1}{m}\sin m\pi\xi\sin m\pi\xi_0\sin\lambda_m x \times\left(1+\frac{2}{\phi_0}\sum_{n=1}^{\infty}\frac{1}{n}\sin n\phi_0\cos n\phi\right) \tag{22}$$

In this case, p_x and p_ϕ in Eq. (10) are zero. Thus

$$\left.\begin{aligned} &X_{nf}(x,\tau)=\Phi_{nf}(x,\tau)=R_{nb}(x,\tau)=0 \quad (n\neq 0)\\ &R_{na}(x,\tau)=p(\tau)\frac{8}{n\pi^2}\sin n\phi_0\sum_{m=1}^{\infty}\frac{1}{m}\sin m\pi\xi\sin m\pi\xi_0\sin\lambda_m x\\ &R_0(x,\tau)=\frac{1}{2}\lim_{n\to 0}R_{na}(x,\tau)\end{aligned}\right\} \tag{23}$$

By substituting Eqs. (19) and (23) in Eq. (14), $Q^{(r)}_{mna}(\tau)$ is determined and then the response function $q^{(r)}_{mna}(\tau)$ is expressed by

$$\left.\begin{aligned} q^{(r)}_{mna}(\tau)&=\frac{8}{\pi^2}\frac{\sin m\pi\xi\sin m\pi\xi_0\sin n\phi_0}{mn(1+\alpha^{(r)2}_{mn}+\beta^{(r)2}_{mn})\omega^{(r)}_{mn}}\int_0^\tau p(\tau')\sin\omega^{(r)}_{mn}(\tau-\tau')d\tau' \quad (n\neq 0)\\ q^{(r)}_{m0a}(\tau)&=\frac{1}{2}\lim_{n\to 0}q^{(r)}_{mna}, \qquad \beta^{(r)}_{m0}=0\end{aligned}\right\} \tag{24}$$

if the initial displacement and velocity of the shell are zero.

When the side pressure is a half-sinusoidal pulse shown in Fig. 4, the function $q^{(r)}_{mna}(\tau)$ is calculated by

$$q^{(r)}_{mna}(\tau)=\frac{F^{(r)}_{mna}}{(\pi/\tau_1)^2-\omega^{(r)2}_{mn}}\left[\left\{\frac{\pi}{\tau_1}\sin\omega^{(r)}_{mn}\tau-\omega^{(r)}_{mn}\sin\frac{\pi}{\tau_1}\tau\right\}u(\tau) +\left\{\frac{\pi}{\tau_1}\sin\omega^{(r)}_{mn}(\tau-\tau_1)-\omega^{(r)}_{mn}\sin\frac{\pi}{\tau_1}(\tau-\tau_1)\right\}u(\tau-\tau_1)\right] \tag{25}$$

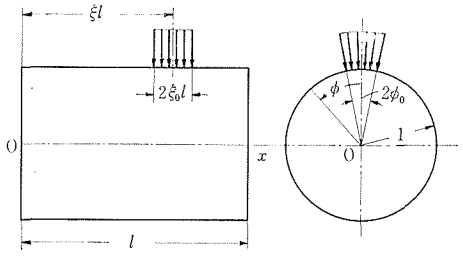

Fig. 3 A side pressure acting on the shell

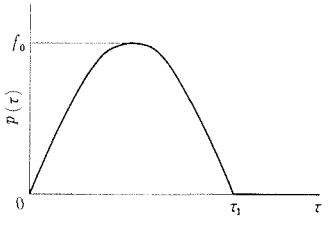

Fig. 4 A half-sinusoidal loading

When the side pressure is a step-load with a straight-line rise as shown in Fig. 5, the function $q^{(r)}_{mna}$ is written by

$$q^{(r)}_{mna}(\tau)=\frac{F^{(r)}_{mna}}{\omega^{(r)2}_{mn}\tau_2}\left[\left\{\omega^{(r)}_{mn}\tau-\sin\omega^{(r)}_{mn}\tau\right\}u(\tau)-\{\omega^{(r)}_{mn}(\tau-\tau_2)-\sin\omega^{(r)}_{mn}(\tau-\tau_2)\}u(\tau-\tau_2)\right] \tag{26}$$

where

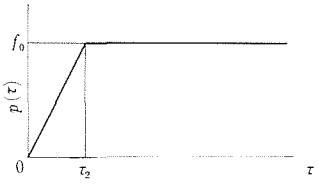

Fig. 5 A step-force with a straight-line rise

$$F^{(r)}_{mna}=\frac{8}{\pi^2}f_0\frac{\sin m\pi\xi\sin m\pi\xi_0\sin n\phi_0}{mn(1+\alpha^{(r)2}_{mn}+\beta^{(r)2}_{mn})\omega^{(r)}_{mn}}\quad(n\neq 0)$$
$$F^{(r)}_{m0a}=\frac{1}{2}\lim_{n\to 0}F^{(r)}_{mna},\qquad \beta^{(r)}_{m0}=0 \tag{27}$$

and $u(\tau-\tau_1)=1$ $(\tau_1<\tau)$, 0 $(\tau<\tau_1)$ is a unit step function.

5. Numerical calculation and experiment

5.1 Convergence of the solution

Since the displacement and stress components are expressed by infinite series, the convergence of which should be checked in the process of numerical calculation. Fig. 6 shows the situation of convergence of the stress components $(\sigma_x)_0$, when one of (m, n) is fixed and the other is varied. In this paper, by taking the values of $(\sigma_x)_0$ obtained for $(m, n)=(100, 1)$ or $(1, 100)$ as the standard, the least number of the terms (m, n) was determined in such a way that the relative error between the value of the finite series with a certain number of terms and the standard value is within $\pm 1\%$. Noting that the infinite series for the displacement converges more quickly than that for the stress, it is considered that a sufficient accuracy of the calculation could be secured.

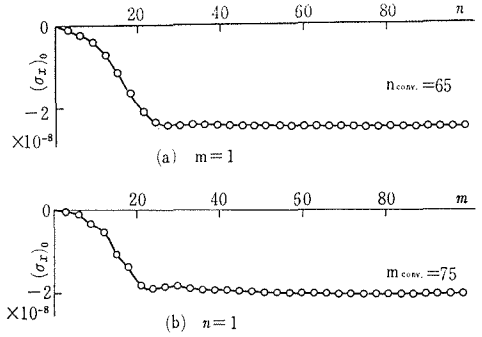

Fig. 6 The convergence of infinite series for $(\sigma_x)_0$ $(x=1.5,\ \phi=0;\ \xi_0=5\times10^{-3},\ \phi_0=5\pi\times10^{-3};\ \tau=3.0)$

5.2 Numerical example

As a numerical example, the response of a circular cylindrical shell $(l=3,\ h=0.01;\ \nu=0.3)$ simply supported at both ends was calculated, when a half-sinusoidal side pressure acts inwards on a square surface area $(|x-1.5|\leq 0.12,\ |\phi|\leq 0.12\approx 7°)$ whose center is located at the midpoint of the cylinder $(x=1.5,\ \phi=0)$.

Figs. 7~9 present the variation of the deflection and the stress at the midpoint and the distribution of them at time $(\tau=3.0)$ produced under the action of the side force $(-f_0=10^{-5},\ \tau_1=\pi)$.

Figs. 7a and 7b show the variation of the lateral deflection w and the normal stress σ_x, σ_ϕ produced at the midpoint. The deflection and stress attain maximum values immediately after the end of loading period, and then the deflection decreases gradually and the stress becomes small at a rapid rate. It should be noted that remarkable deformation and stresses occur within the double loading period. On the inner surface $(z=-h/2)$, tensile stress

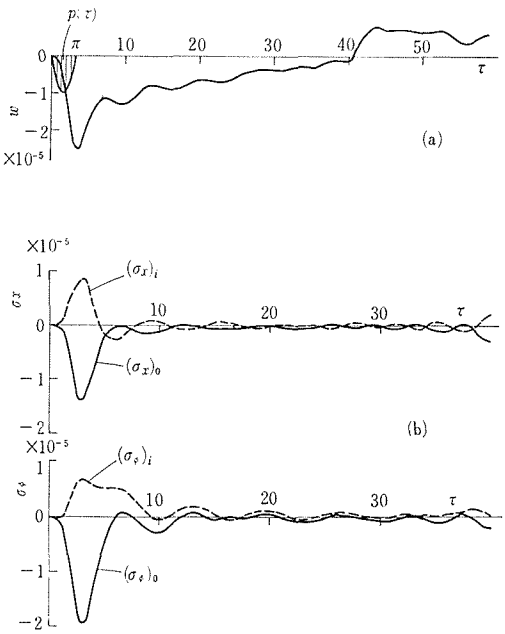

Fig. 7 The variation of lateral deflection and stress components $(x=1.5, \phi=0)$

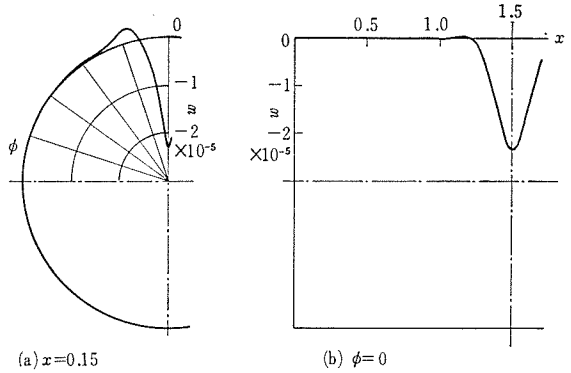

(a) $x=0.15$ (b) $\phi=0$

Fig. 8 The distribution of deflection in thes ymmetrical plane and the circular section ($\tau=3.0$)

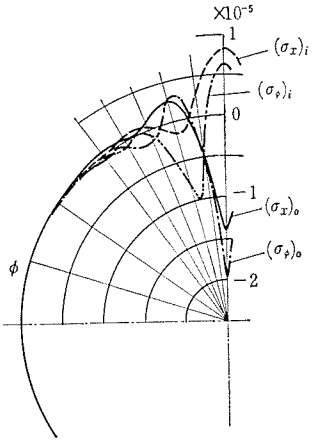

(a) $x=0$

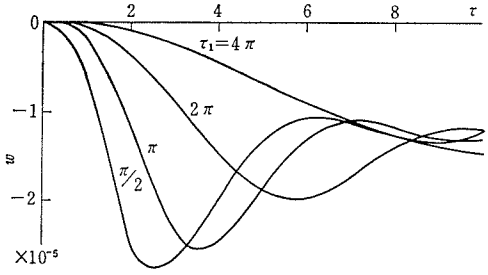

Fig. 10 The variation of lateral deflection ($x=1.5$, $\phi=0$)

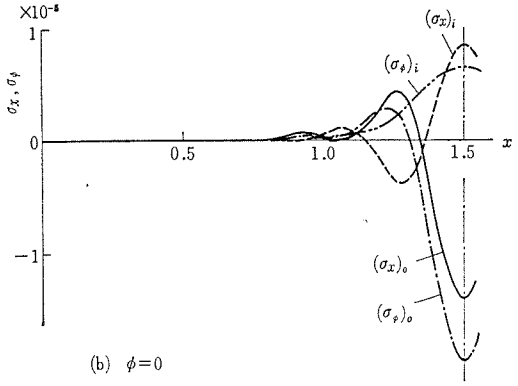

(b) $\phi=0$

Fig. 9 The distribution of stress components in the symmetrical plane ($\tau=3.0$)

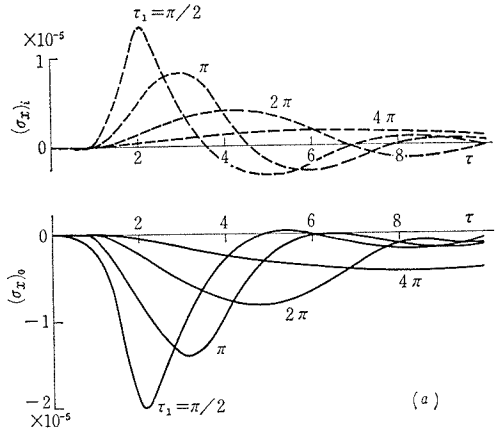

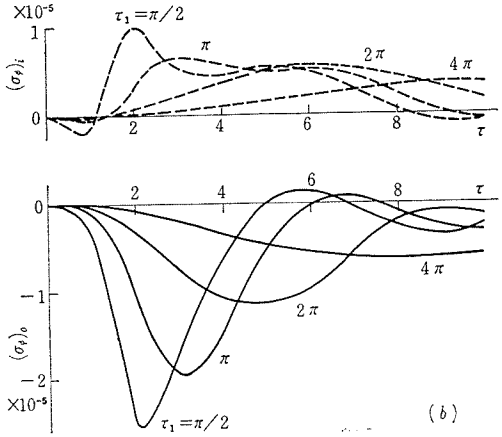

Fig. 11 The variation of sress components ($x=1.5$, $\phi=0$)

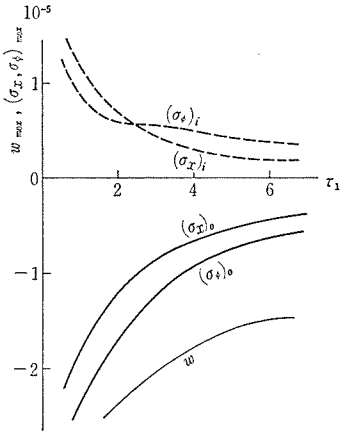

Fig. 12 The maximum values of deflection and stress components ($x=1.5$, $\phi=0$)

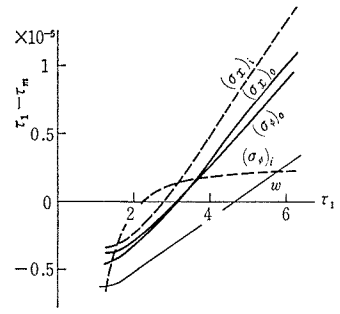

Fig. 13 The relation of duration of loading and the time producing the maximum deflection and stress ($x=1.5$, $\phi=0$)

$(\sigma_x, \sigma_\phi)_i$ is caused and on the outer surface ($z=h/2$), compressive stress $(\sigma_x, \sigma_\phi)_0$ is caused at the beginning. The compressive stress is larger than the tensile stress and almost $|(\sigma_x)_0|=1.7\,|(\sigma_x)_i|$, $|(\sigma_\phi)_0|\approx 3\,|(\sigma_\phi)_i|$. Either of displacement components u, v and shearing stress $\tau_{x\phi}$ do not occur at the midpoint.

Figs. 8 and 9 show the distribution of the deflection and the normal stress, which are produced in the symmetrical plane and the circular section including the loading point at the time $\tau=3.0$ when large stresses occur. Compressive stress occurs on the outer surface and tensile stress occurs on the inner surface within the narrow surface $|x-1.5|<0.15$, $|\phi|<7°$ at $\tau=3.0$. Although the stresses may turn over outside of the range and in course of time, the stress level decreases rapidly. However, it should be noted that remarkable stresses occur within the range of two or three fold on the loading surface.

Figs. 10 and 11 present the variation of the lateral deflection and the normal stress produced at the midpoint under the action of half-sinusoidal pressure with various loading periods τ_1. In this case, the maximum value f_0 of loading is chosen for each τ_1 so that a constant impulse is always given to the shell surface. Fig. 12 shows the maximum values of the deflection and stress and Fig. 13 shows the difference between time τ_m at which time the maximum values occur and the loading period, by taking τ_1 as the axis of the abscissa. The shorter the loading period becomes, the larger the deflection and the stress level is. And when the loading period is short, the time causing the maximum stress becomes fast and occurs during loading. This fact is considered to result from the inertia of the shell.

5.3 Experimental result

An experiment was conducted on a steel circular cylinder ($l^*=662$, $a^*=106$, $h^*=5.5$ mm) by using an impacting hammer (5□mm) shown in Fig. 14. The strain components were measured at several points on the cylinder surface and the side pressure was estimated by transducing the strain detected with a pick up. The measured side force was almost similar to a half-sinusoidal wave, which was expanded into Fourier series as inputs of the computer.

Fig. 15 shows the variation of the stress measured at a point ($|x/l-0.5|=0.03$, $|\phi|=0.06\approx 3.5°$) on the outer surface of the cylinder loaded at midpoint and the results obtained by the theoretical calculation. The theoretical values of the

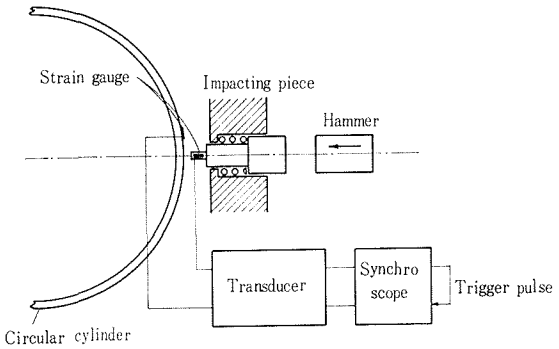

Fig. 14 The apparatus of experiment

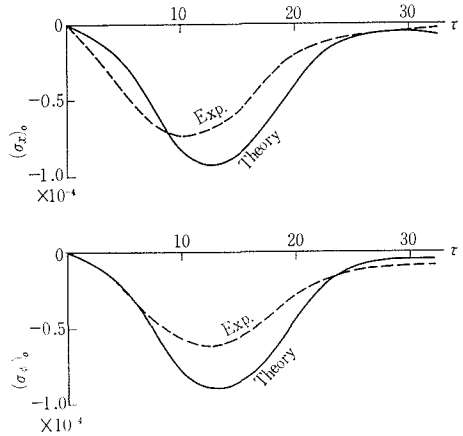

Fig. 15 The result of theoretical calculation and experiment on stress components ($\xi=0.5$, $\phi=0$; $\xi_0=0.008$, $\phi_0=0.008\simeq 0.5°$)

maximum stress are larger than the experimental one by 25～45%. The reason is explained from the fact that completely simple supports of the cylinder could not be made, thus side pressure loaded by a hammer might not be uniformly distributed on the surface and moreover damping of the cylinder was not taken into consideration.

6. Conclusions

A theory was developed on the dynamic response of a thin cylindrical shell to side pressure acting on a narrow surface and the following results were obtained.

(1) The response function was obtained by Fourier series in the general form, which can be applied to any transient loading under arbitrary boundary conditions.

(2) The dynamic response was calculated numerically in the case where a half-sinusoidal load acted on the shell simply supported at both ends.

(3) The maximum deflection and stresses occur immediately after the end of loading and remarkable deformation and stresses are caused in a range of two or three fold loaded surface during the double loading period.

(4) When the loading period becomes short, the deflection and stress levels increases and the time at which the maximum stresses occur becomes fast.

(5) The result of the theoretical calculation qualitatively agrees with that of the experiment conducted on a steel cylinder.

References

1) Lord Rayleigh, Proc. Roy. Soc., 45 (1889), p. 113 & p. 443.
2) Love, A. E. H., Phil. Trans. Roy. Soc., A179 (1888), p. 538.
3) Flügge, W., Statik und Dynamik der Schalen, (1935), p. 268, Springer.
4) Donnel, L. H., NACA TR 479 (1933).
5) Arnold, R. N. and Warburton, G. B., Proc. Roy. Soc., A197 (1947), p. 238.
6) Arnold, R. N. and Warburton, G. B., Proc. Inst. Mech. Engrs., 167 (1953), p. 62.
7) Baron, M. L. and Bleigh, H. H., J. Appl. Mech., 21 (1954), p. 167.
8) Yu, Y-Y., J. Appl. Mech., 22 (1955), p. 547.
9) Yu, Y-Y., J. Aerospace. Sci., 25 (1958), p. 669.

10) Forsberg, K., AIAA J., 2 (1964), p. 2150.
11) Humphreys, J. F. and Winter, R., AIAA J., 3 (1965), p. 27.
12) Sheng, J., AIAA J., 3 (1965), p. 701.

The authors wish to thank the Computing Center of Hokkaisdo University, for providing the facilities and valuable cooperation whithout which the present calculations could not be made.